Journal of Food Engineering 406 (2026) 112798

Contents lists available at ScienceDirect

Journal of Food Engineering

journal homepage: www.elsevier.com/locate/jfoodeng

Multi-wavelength laser texturization with 3D-printed foods

Jonathan David Blutinger [a,b,c,*], Evan Lloyd Omo [a], Pol Bernat [a], Hod Lipson [a]

[a] Department of Mechanical Engineering, Columbia University in the City of New York, 500 West 120th St., Mudd 220, New York, NY, 10027, USA
[b] Redefine Meat Ltd., Prof. Hillel ve-Khanan Oppenheimer St 10, Rehovot, 7670110, Israel
[c] U.S. Army DEVCOM Soldier Center, General Greene Ave, Natick, MA, 01760, USA

ARTICLE INFO

Keywords:
3D food printing
Additive manufacturing
Laser cooking
Food texturization
Thermal processing
Multi-material

ABSTRACT

Organoleptic evaluation plays a crucial role in our perception of food. Our sensory experiences are not solely determined by taste, but rather by the integrated inputs from all of our senses—taste, sight, smell, hearing, and touch. Multi-ingredient food printing is an emerging technology that enables the creation of novel flavors and unique food combinations. While this technology shows potential for developing customized, nutritious meals and plant-based meat analogues, it faces challenges in replicating textures that are perceived as 'crunchy' or firm, which are key factors influencing consumer acceptance. This study investigates the use of blue (λ = 445 nm), near-infrared (λ = 980 nm), and mid-infrared (λ = 10.6 μm) lasers as thermal processing tools for texturizing 3D-printed foods *in situ*. We found that modulating the frequency of laser exposure across printed layers allows for precise control over elasticity and chewiness throughout the printed product. Firmer textures were achieved with more frequent laser exposure, and compression testing validated that laser-cooked samples exhibited peak elasticity at mid strain (5%–10%), while oven-baked samples were firmer at high strain (20%–30%). Additionally, we demonstrate *in situ* cooking of a complex, multi-ingredient 3D-printed three course meal (14 ingredients). Our findings highlight the importance of controlling food texture to enhance the sensory experience of 3D-printed foods, which remains a critical challenge for broad consumer adoption.

1. Introduction

Our first impressions of food are heavily influenced by visual aesthetic and color (Spence et al., 2022; Suzuki et al., 2017; Tang et al., 2014), but texture and flavor often play an even more critical role in determining an individual's preference for a food product (Pellegrino and Luckett, 2020; Jeltema et al., 2016). Texture, in particular, is a key factor (Pellegrino and Luckett, 2020; Christensen, 1984; Jaworska and Hoffmann, 2008; Wilkinson et al., 2000), which for printed foods, is largely limited to pastes (Liu et al., 2017; Hertafeld et al., 2019; Blutinger et al., 2021; Zoran, 2019), liquids (De Grood and De Grood, 2013; Willcocks et al., 2011), and powders (Gray, 2010). Due to the implicit liquid-like flow characteristics of 3D-printable formulations (Cheng et al., 2022; Maldonado-Rosas et al., 2022), controlling texture for 3D-printed foods is especially important for consumer acceptance (Huang et al., 2019; Stokes et al., 2013). Foods that exhibit crunchy, brittle, or firm textures require additional post-processing after printing (Noort et al., 2017; Renzetti and Jurgens, 2016). Achieving these textures during printing remains a challenge, driving the development of innovative technologies like laser cooking (Blutinger et al., 2018; Fukuchi et al., 2012). With its tunable heating capabilities, laser cooking aims to meet consumer expectations by replicating the sensory qualities of traditional cooking while enabling personalization.

Since 2007, additive manufacturing (AM) of food has progressed from printing with one ingredient (Periard et al., 2007), to printing with multiple ingredients (Hertafeld et al., 2019), to printing and cooking with lasers in tandem (Blutinger et al., 2021, 2023, 2024). These hardware developments, accompanied by improvements in software, have expanded the applications of this technology to include plant-based meat replication (Meat, 2025; Foods, 2023), medical drug release (Zhang et al., 2021), customized vitamins (Vitamins, 2025), cake decorating (Automation, 2025), chocolate printing (Edge, 2021; Press, 2025), pasta printing (Egbert-Jan et al., 2015), and ice cream mold-making (Pops, 2022). In each of these applications, desired food textures are achieved with some form of post processing or food phase-change due to cooling or heating of the substrate. To achieve variable texture within the same food product, however, a precise targeted heat source is required to enable controlled cooking.

One possible solution to this problem is to vary the infill structure to create a different mouthfeel and perceived texture in the food (Derossi et al., 2021). Alternatively, thermal processing can be used since—aside from the nutritional changes that may result—it tends to cause textural

* Corresponding author at: U.S. Army DEVCOM Soldier Center, General Greene Ave, Natick, MA, 01760, USA.
E-mail address: jdb2202@columbia.edu (J.D. Blutinger).

https://doi.org/10.1016/j.jfoodeng.2025.112798
Received 27 June 2025; Received in revised form 27 August 2025; Accepted 28 August 2025
Available online 13 September 2025

Table 1
Food formulations for the printed courses, with ingredients grouped by sequentially numbered food "inks" (or *f.inks*). A total of 14 f.ink cartridges were used for the print.

Course	Ingredients by F.ink
Appetizer	**F.ink 1 (Base)**: 140 g Carr's Rosemary Crackers, 2.5 tbs. Butter, 55 g Water **F.ink 2 (Filling)**: 55 g Just Egg, 225 g Spinach (dried), 225 g Heavy Cream, 8 oz. Mascarpone Cheese **F.ink 3 (Topping 1)**: 225 g Mushrooms (dried), 30 g Sour Cream **F.ink 4 (Topping 2)**: Pinch of Salt **F.ink 5 (Topping 3)**: Pinch of Pepper
Main	**F.ink 6 (Base)**: Cauliflower Dough **F.ink 7 (Filling)**: Tomato Paste **F.ink 8 (Topping 1)**: Ricotta Cheese **F.ink 9 (Topping 2)**: Basil Pesto **F.ink 10 (Topping 3)**: Parsley Flakes
Dessert	**F.ink 11 (Base)**: 140 g Graham Crackers (8 sheets), 2.5 tbs. Butter, 85 g Water **F.ink 12 (Filling)**: Key Lime Pie Filling, 55 g Just Egg, 70 g Water **F.ink 13 (Topping 1)**: Frosting (green) **F.ink 14 (Topping 2)**: Whipped Cream

and visual changes in foods as well (Almeida and Chang, 2013; Nashat and Abdullah, 2016; Ahrné et al., 2007). Bulk heating with stovetops, ovens, or grills do not lend themselves well, however, to printed foods since their heating is fairly low resolution (Datta and Rakesh, 2013) and cannot be controlled with millimeter precision. Conversely, lasers offer exceptional versatility as a heating method since they offer high resolution heating at shallow penetration depths (Blutinger et al., 2019a,b, 2021) yet the resultant textural changes of laser-heated foods have not been analyzed.

In this study, we investigate the textural changes in 3D-printed foods processed with lasers and compare them to conventionally cooked samples (Supplementary Video 1). Using graham cracker paste as a model food system, we assess changes in material elasticity caused by blue lasers (λ = 445 nm), near-infrared lasers (λ = 980 nm), and mid-infrared lasers (λ = 10.6 μm), alongside an oven-baked reference sample. Finally, we demonstrate the versatility of 3D food printing and laser processing by designing, printing, and cooking a full-course meal consisting of 14 unique ingredients (Supplementary Video 2)—as far as the authors are aware, the most ingredients ever printed in a single food product, surpassing the previous record set in prior work (Blutinger et al., 2023).

2. Materials & methods

2.1. Sample preparation

All ingredients used for printing were sourced from a local bodega (Appletree Market, New York City, USA) or a grocery store (Whole Foods Market, Austin, Texas, USA) and prepared using either a Food Processor (Cuisinart, Stamford, Connecticut, USA) or high-powered Blender (Vitamix, Olmsted Falls, USA). Table 1 provides an itemized list of the ingredients for each of the three courses. A total of 14 unique food "inks"—also referred to as *f.inks*—(pastes and powders) were used for this print.

The appetizer was inspired by a quiche. The crust was created with a mixture of 140 g of Rosemary Crackers (Carr's, Carlisle, United Kingdom), 2.5 tbs. of butter, and 55 g of water. These were blended in a food processor until a creamy texture was achieved. The internal mixture consisted of 55 g of Just Egg (Eat Just, San Francisco, California, USA), a vegan alternative to regular eggs, blended with fresh spinach and heavy cream; this mixture needed to be blended until the spinach fibers were broken down to prevent nozzle clogging. Mascarpone (cheese) was the final ingredient added to this mixture. This mixture was used as a filling, which rested in the laser-crusted exterior. The residual liquid from a handful of white mushrooms was mixed into sour cream and dolloped atop the structure, along with a pinch of salt and pepper.

Gluten-rich ingredients can often be difficult to extrude due to their elasticity, which is why we opted for an organic cauliflower dough (Navitas, Novato, California, USA) as the base for our main course (inspired by a pizza). Additionally, a recipe using fresh mozzarella was attempted, but it was difficult to extrude due to clumping. Ingredient toppings used in the final print included tomato paste, ricotta (cheese), basil-pesto, and parsley flakes.

Our printed dessert was inspired by a key lime pie. The crust followed the same recipe as the quiche crust, substituting Honey Maid Graham Crackers (Nabisco, East Hanover, New Jersey, USA) for the Rosemary Crackers to give it a sweeter taste. A Key Lime Pie Filling mixture (Dr. Oetker, Bielefeld, Germany), combined with Just Egg and water, was used to create the filling layers, based on the recipe from the dessert mix. Freshly whipped cream and some green frosting was used to make the intricate lime pattern atop the filling.

2.2. Food design

Similar to conventional cooking, a successful 3D-printed food design considers many factors, such as structure, aesthetics, and flavor profiles. The motivation behind our 3-course meal was to showcase a variety of ingredients that can be printed, while creating foods that look appetizing and palatable. The printed courses were inspired by a spinach-mushroom quiche (appetizer), a margherita pizza (main), and a key lime pie (dessert). Each course was chosen for its variety of ingredient textures, compositions, colors, and flavors. Fig. 1 shows the CAD assembly design of the full print.

Typical additive manufacturing (AM) requires support material to achieve complex three-dimensional structures. Conversely, food AM designs must consider food rheology and viscoelastic properties for structural stability (Blutinger et al., 2023). To print with softer ingredients, such as jellies or pudding, we found success with dish designs that use stronger materials to first create a structure into which the softer ingredients are deposited. The quiche portion of our design uses a savory cracker paste to form a bowl shape with a 45° inner taper. The paste is then cooked with a blue laser (λ = 445 nm) to stiffen its structure. Once the cracker-paste crust is printed, the softer spinach-cheese-egg mixture is deposited onto it. Fig. 1 shows an exploded CAD view of the quiche layers. Note that in the actual print, the egg, spinach, and mascarpone are combined into a variegated mixture to better resemble a traditional quiche dish.

The margherita pizza and key lime pie are designed with a similar philosophy. The pizza uses dough to create a shallow cavity for the tomato sauce filling. The cheese topping layered on top also has built-in cavities to hold tomato dollops. The structure and layering give the pizza a more natural appearance in the final print.

Similar to the quiche, the key lime pie uses a sweet cracker paste for the crust. The layer frequency of laser cooking allows us to control the texture of the crust, making it soft or chewy depending on the cooking process. For example, if the crust is laser-cooked after each printed layer, it will be chewier than if it is cooked every two or three layers. The key lime pie filling also exhibited better cohesive strength than the quiche mixture, and the crust was designed to be open on two sides, more closely resembling a traditional pie slice.

2.3. Printing and cooking apparatus

An off-the-shelf Cartesian screw gantry was purchased (Alibaba Group, Hangzhou, China) and retrofitted with a custom-designed extrusion head and tool rack for the automated swapping of ingredient cartridges. All motion axes were driven by ClearPath brushless servomotors (Teknic, Inc., Victor, New York, USA) and controlled by a

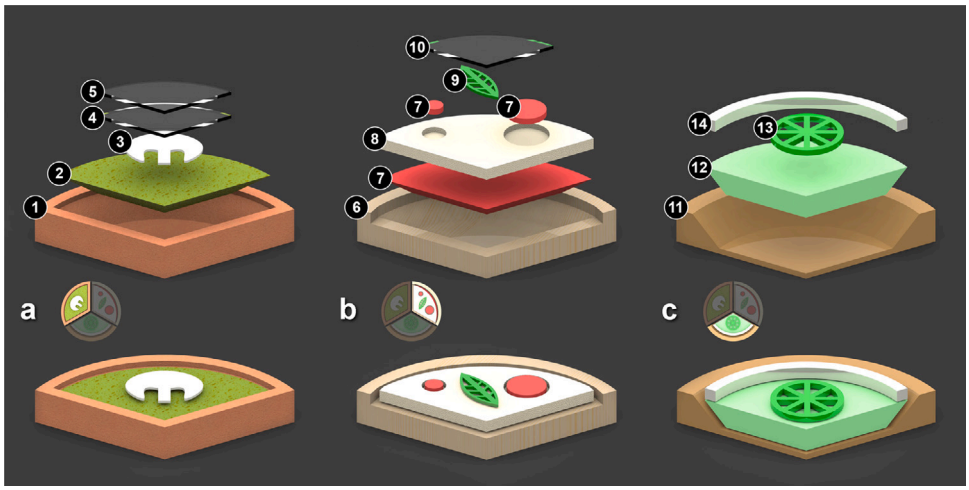

Fig. 1. Computer-aided design models of the 3-course meal. The upper image presents an exploded view of the fully assembled course below. The (a) appetizer consists of a (1) savory crust, (2) spinach-egg cream mixture, (3) mushroom-sour cream, (4) salt and (5) pepper. The (b) main course included (6) dough, (7) tomato paste, (8) ricotta, (9) pesto, and (10) parsley. The (c) dessert includes a (11) sweet crust, (12) key lime filling, (13) frosting, and (14) whipped cream.

Duet 2 WiFi board, an open source hardware platform used to drive 3D printers. Our extruder accommodates custom-printed cartridges that house a 30 mL syringe barrel (PN: 7012134) and a 14-gauge flexible nozzle tip (PN: 7018052).

Cooking was carried out with a variable power blue laser (similar to the one used by Blutinger et al. (2021)). The power for the blue laser was set to 5 W for all of the experiments. Two other lasers were used for the texture analysis trials: (1) a near-infrared (NIR) laser operating at a wavelength of 980 nm and a power of 8 W, and (2) a mid-infrared (MIR) laser operating at 10.6 μm and a power of 8 W.

2.4. Texture analyzer

Similar to our custom food printer, we used another off-the-shelf Cartesian screw gantry (Alibaba Group, Hangzhou, China) with custom hardware to create a high-fidelity compression testing machine. This machine features a 3-axis force gauge (PN: FNZ-20N) and load cell amplifier (PN:LC3A(−10–10 V)–24 V) (Forsentek Co., Hangzhou, China) to capture texture data on food samples. Information from the load cell is recorded via USB Data Acquisition (USB-6009) (National Instruments, Austin, Texas, USA) and read directly into MATLAB (Mathworks, Natick, Massachusetts, USA) for efficient data capture.

A custom laser-cut mount was designed for the load cell to accommodate various attachments for "poking" food products for texture analysis. Using a 1/8″ in stainless steel dowel rod as an end-effector for the load cell, we crafted a 10 mm diameter circular attachment to place at the end of this rod. The flat circular attachment was 3D-printed out of PLA (visible in Fig. 2a) and mounted to the pushing dowel.

2.5. Compression testing

Graham cracker paste (Ink 11 from Table 1) was selected to investigate laser-induced textural changes. Rectangular samples (approximately 50 mm × 20 mm × 10 mm) were 3D-printed and served as test specimens for compression analysis. Each sample underwent three separate compression tests, spaced 15 mm apart (center-to-center) to avoid any overlap or interference from previous tests. The laser wavelength and layer frequency were varied for each exposure to assess their impact on textural properties. All experiments were conducted in triplicate to ensure reproducibility, producing three identical samples for comparison and analysis. Fig. 2a shows a food sample before and after compress ion testing.

2.6. Machine calibration

Various known masses (10 g to 1 kg) were fixed to the end of the poking tool and the voltage reading was measured. This was done for each of the axes. The X and Y axes required the use of a pulley system such that the force created by the masses was at a right angle to the Z axis. A linear regression was performed on the captured voltage data at distinct force measurements and converted into equations for each axis of motion (Eqs. (1), (2), and (3)). This allowed us to determine the force applied by the load cell based on a given voltage.

$$F_x = \frac{(V_x + 1.32)}{0.36} \tag{1}$$

$$F_y = \frac{(V_y + 1.35)}{0.382} \tag{2}$$

$$F_z = \frac{(V_z + 1.41)}{0.483} \tag{3}$$

2.7. Data processing

Raw data from the load cell came in the form of a continuous data stream of force in the X, Y, and Z direction. Additionally, output from a limit switch was recorded that was triggered each time the load cell was moving downward to engage with the food sample. Because the machine is "open-loop", this piece of information was crucial for determining the thickness and extent of the strain exhibited by the food sample for each sampling.

Various scripts were written to gather elasticity data from the compression analysis. Force data was captured in all three axes of motion, but the Z axis information was used primarily to calculate the local Young's modulus (Eq. (4)). As soon as the force changed by some user-inputted threshold, this point was registered as l_0 and $F = 0$. From this point forward, an increase in force was registered as strain progressed linearly in the Z axis. The area (A) corresponds to the pushing arm circle.

$$E = \frac{\sigma}{\epsilon} = \frac{F/A}{\delta l/l_0} \tag{4}$$

2.8. Statistical analysis

To evaluate the mechanical differences between different thermal processing methods, we analyzed the Young's modulus of the various methods across four distinct regions (2%–5%, 5%–10%, 10%–20%,

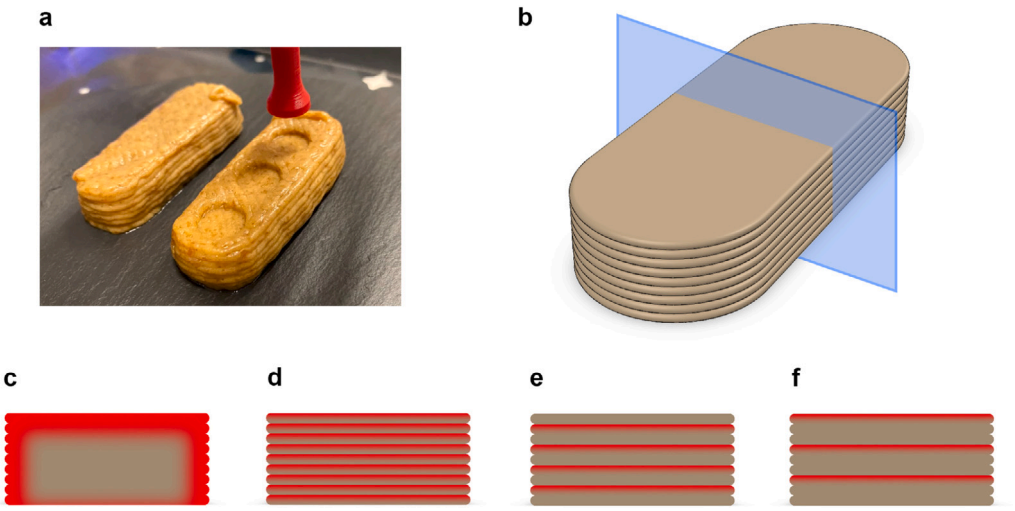

Fig. 2. Compression analysis and thermal processing schematic. **a** A 3D-printed graham cracker sample before (left) and after (right) compression testing. **b** A 3D model of the graham cracker sample showing a cross-sectional cut (blue shaded plane). Each cross-sectional cut from **b** is shown with the approximate heat distribution (shown in red) from (**c**) oven heating, (**d**) laser heating every layer, (**e**) laser heating every two layers, and (**f**) laser heating every three layers.

and 20%–30% strain) using a one-way ANOVA followed by Tukey's HSD post-hoc test. Each thermal processing method was repeated in triplicate using printed food models (n = 3), and within each sample, three compressive tests were conducted at different locations to account for spatial heterogeneity (Fig. 2). Results from the ANOVA test showed statistically significant differences across cooking methods in all four strain regions ($p < 0.0001$ for each), indicating that cooking method has a measurable impact on elasticity. Additionally, the one-way ANOVA proved that repeated trials of the same cooking test on different food models revealed no significant differences among samples that were cooked using the same heating conditions.

3. Results and discussion

Thermal processing of dough products often induces textural changes (Faridi and Faubion, 2012), which vary depending on exposure time and the depth of heat penetration. As part of our comparative analysis, we exposed graham cracker paste to blue light, near-infrared (NIR) light, and mid-infrared (MIR) light at varying levels of exposure. For each laser type, scan patterns and speeds were kept constant, while the interval of layers between cooking cycles was adjusted. This modulation of layer intervals enabled precise control over the textural properties of the 3D-printed food structures while ensuring relatively uniform heat distribution.

3.1. Laser-induced food texturization

Baseline measurements indicated that raw, 3D-printed graham cracker samples exhibited an elasticity range of 2–17 kPa across all strain regions (Table 2). These raw samples were stiffer at lower strains and softer at higher strains (Fig. 3H and I). Although dehydration slightly increased stiffness, it did not significantly alter mechanical properties. However, heating caused a distinct shift in these patterns. Oven-baked samples displayed a progressive increase in stiffness with strain, reaching a maximum elasticity of 245.1 kPa at high strain levels (20%–30%). These samples, baked at 365°F for 10 min in a convective toaster oven, experienced sufficient dehydration and stiffening. This pronounced increase in $\overline{E}$ suggests robust structural reinforcement due to starch cross-linking, protein denaturation, and sugar caramelization (Mondal and Datta, 2008; Scanlon and Zghal, 2001). Collectively, these processes yield a more rigid and homogeneous structure resistant to deformation.

In the low to moderate strain range (2%–20%), laser-cooked graham cracker samples achieved stiffness values comparable to oven-baked counterparts. Notably, at strains below 10%, laser processing demonstrated particularly high stiffness, though this may be partially attributed to differences in oven settings used during comparative tests. More broadly, the highest stiffness for laser-cooked samples was observed in the mid-strain region (5%–10%), potentially due to more evenly distributed layer heating.

Oven-based heat propagation differs fundamentally from irradiated heat within additively manufactured food products (Datta and Rakesh, 2013) (illustrated in Fig. 2). Oven heating primarily relies on hot-air convection and is controlled by two main variables—temperature and time—to achieve the desired level of "doneness". In contrast, laser cooking offers multi-dimensional thermal control, allowing for the precise tuning of parameters such as power, exposure time, cooking path, wavelength, laser flux, and—specific to this context—layer frequency. Limitations in laser cooking heat penetration depth can be mitigated by adjusting the frequency of laser-cooked layers, as depicted in Fig. 2.

3.2. Energy thresholds for food texturization

For the strain regions measured, there was a direct correlation between total energy input and the elastic modulus, particularly for laser-cooked samples. A clear energy threshold appears to be necessary to induce significant structural changes, such as stiffening or cross-linking. "Noticeable textural changes" were defined as a fivefold increase in elasticity compared to the raw food product (control). For low to moderate strain, a total energy input of ≥3 kJ was required to achieve such changes, while high strain levels necessitated upwards of 4 kJ. These findings are visualized in Fig. 4, which presents distilled data from Table 2.

To further illustrate these thresholds, we classified the laser cooking trials into three energy categories: low energy (0–2 kJ), moderate energy (2.1–4 kJ), and high energy (4.1–6 kJ). Low energy trials resulted in minimal structural changes, likely due to insufficient energy to initiate significant cross-linking or dehydration. Moderate energy exposure promoted structural reinforcement, with stiffness increases observed predominantly in the low and mid-strain regions, likely due to localized cross-linking and dehydration. High energy trials exhibited pronounced increases in stiffness across all strain regions, peaking in the mid-strain range. The observed decrease in elasticity at higher strains may indicate a dominance of localized stiffening (e.g., crust formation) that is insufficient to maintain rigidity under high deformation.

Table 2
Local elasticity (Young's modulus, E) measurements for different strain regions, obtained via compression testing using a 10 mm diameter probe. Graham cracker samples experienced mild plastic deformation during testing. The color of the laser light as well as the frequency of the cook cycles is noted in the left column (e.g., "Blue per 3L" denotes that a blue laser was used every three print layers). For the samples listed as "Raw", the time denotes how long they were left out before testing. Standard error (SE) measurements are calculated from the error in the slope calculations for $\overline{E}$. As a more useful means of comparison, laser processing methods are organized in order of increasing total laser energy supplied to the food sample.

Thermal processing method	Total laser energy	Low strain (2%–5%)		Mid strain (5%–10%)		Moderate strain (10%–20%)		High strain (20%–30%)	
	[kJ]	$\overline{E}$ [kPa]	SE [kPa]	$\overline{E}$ [kPa]	SE [kPa]	$\overline{E}$ [kPa]	SE [kPa]	$\overline{E}$ [kPa]	SE [kPa]
Raw, 15 min	–	12.6	0.10	8.3	0.08	4.7	0.03	2.4	0.02
Raw, 30 min	–	16.8	0.13	10.5	0.07	5.4	0.05	2.4	0.02
Oven	–	43.9	0.99	109.1	0.79	197.5	0.97	245.1	0.15
MIR on top L	1.0	7.4	0.01	7.97	0.01	5.7	0.02	6.7	0.08
Blue per 3L	2.0	30.6	0.05	31.9	0.02	25.7	0.09	18.5	0.10
Blue per 2L	2.6	46.9	0.37	56.1	0.06	51.9	0.24	35.0	0.13
NIR per 3L	3.1	82.0	0.80	106.7	0.07	73.4	0.50	19.4	0.39
NIR per 2L	4.2	98.5	1.40	157.4	0.15	112.9	0.62	44.8	0.44
Blue per 1L	5.9	148.7	2.38	204.6	0.97	196.8	0.63	131.2	0.32

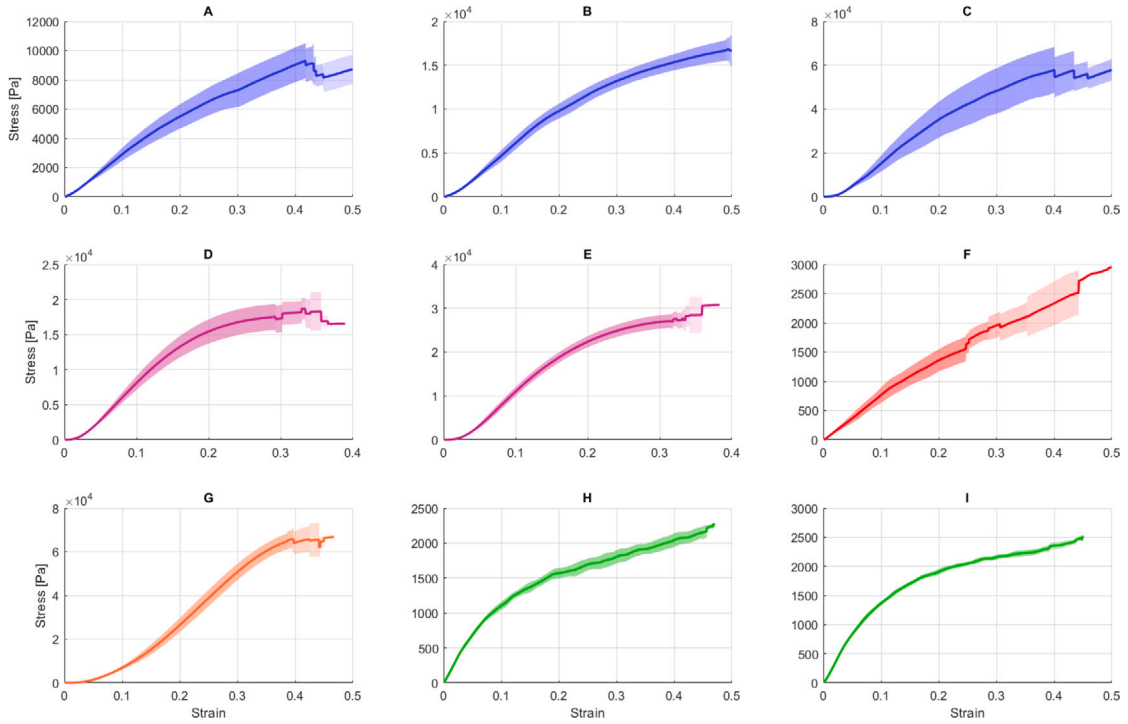

Fig. 3. Stress–strain data from compression testing of thermally processed food samples with a graham cracker structure subjected to various cooking methods. Results are presented for: a blue laser applied in increments of (A) three layers, (B) two layers, and (C) one layer; an NIR laser applied in increments of (D) three layers and (E) two layers; an (F) MIR laser applied to the top surface; and (G) a convection oven. Additionally, raw control samples were tested after being left out for (H) 15 min and (I) 30 min. The shaded regions around each curve represent the 95% confidence interval, with darker regions indicating segments where more data contributed to the calculation.

These energy thresholds are highly dependent on the geometry of the food sample being cooked. Considering the rectangular shape of the bar (Fig. 2b), with an approximate total volume of 9.1×10^{-6} m^3, and the energy requirements for pronounced food texturization (3–4 kJ), the calculated requirement for texturization is approximately 330–440 MJ/m^3. Additionally, the laser parameters differed slightly across trials, with the MIR and NIR lasers operating at 8 W and the blue laser at 5 W. Variations in beam flux and wavelength could also influence the efficiency of laser-induced textural changes.

Oven-cooked samples, likely exposed to higher total energy inputs, exhibited much greater stiffness across all strain regions. This is potentially due to the uniform heating provided by convective oven heating over a longer duration, facilitating more extensive cross-linking and moisture loss. Fig. 2c illustrates heat dispersion in an oven-cooked sample, compared to Fig. 2d, e, and f, which depict heat dispersion from laser cooking. These differences in thermal propagation likely account for the observed disparities in elasticity across strain regions.

Despite delivering highly localized energy, pulsed heating often results in less uniform textural changes because the energy is concentrated on selective printed layers and may not penetrate deeply enough to achieve the same degree of textural transformation. While laser-irradiated food may exhibit lower stiffness than oven-baked food in certain strain regions, laser processing nevertheless demonstrates significant increases in elasticity with relatively small increases in energy input.

3.3. Practical demonstration: printing a three-course meal

Up to this point, our investigation of laser cooking technology has focused on texturization using single-ingredient printing. However, to fully explore its potential applications, we extended this work to

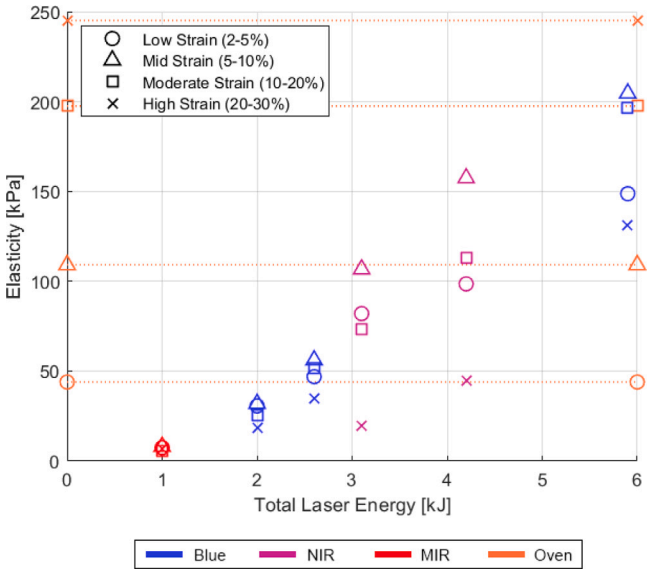

Fig. 4. Elasticity as a function of total laser energy. Icons are colored based on the laser that was used for cooking at the particular total energy (visible in the legend below the graph). The dotted orange lines mark the strain regions for oven-cooked samples, which can be used as a reference.

a practical demonstration by designing and assembling a fully 3D-printed, selectively cooked three-course meal (Fig. 5). This meal was composed of 14 distinct food formulations, or "f.inks", as detailed in Table 1. Except for three solid ingredients (salt, pepper, and parsley), all f.inks were prepared as pastes. Drawing inspiration from previous work (Blutinger et al., 2023), we strategically arranged the ingredients to optimize structural stability and functionality. Thicker f.inks served as foundational elements for crusts and exterior supports, while softer, shear-thinning formulations were utilized as fillings to enhance layering and cohesion.

Visual perception of the printed food is a critical factor for consumer acceptance of this technology (Spence et al., 2022). Earlier iterations of the three-course meal featured extruded circular bites stacked and layered in a way that obscured distinctions between courses (Supplementary Video 2). For example, respondents in a casual survey struggled to differentiate the quiche-inspired appetizer from the ratatouille-inspired main course. While vibrant colors can evoke associations with healthy ingredients (Spence et al., 2022), the visual appeal and flavor of the printed food must also align with consumer expectations. Additionally, portion size was a key consideration; the earlier designs were overly large and lacked the visual engagement achieved by the final design (Fig. 5), which divides a circular format into distinct thirds for each course.

A notable advantage of in situ thermal processing of 3D-printed foods is the ability to retain the shape of softer ingredients after cooking (Zhang et al., 2022). Raw printed ingredients tend to deform as successive layers are deposited, as shown in Fig. 6a and b, where the graham cracker paste visibly sags without cooking. The weight of upper layers often causes lower layers to buckle or bulge under stress (Cheng et al., 2023; Zhu et al., 2019). However, tandem laser cooking on a multi-layer basis induces sufficient stiffening of ingredients, allowing them to maintain their structural integrity and shape during printing (Fig. 6c and d). This feature provides greater design flexibility, enabling the creation of complex and visually appealing food geometries.

Another valuable feature of laser cooking is the ability to selectively cook specific layers while leaving other components raw (Blutinger et al., 2024). This selective processing enables the fortification of certain elements of a printed structure to ensure that the final product adheres to its digital twin. Additionally, laser-cooked food exhibits minimal shape changes post-cooking, an attribute previously observed with mid-infrared lasers in similar contexts (Blutinger et al., 2019a).

3.4. Limitations and future work

A few inherent limitations of this study pertain to the laser cooking apparatus, the model food system used for experimentation, and the overall study design. First, the time-intensive nature of each cooking trial made testing all samples in triplicate a laborious task. Consequently, we prioritized repeated trials across a narrow range of thermal processing conditions, rather than a broad exploration of laser parameters with singular cooking trials. Second, the use of a single model food system limits the extensibility of the observed laser-induced textural changes to other foods. Ingredients with differing macro- and micronutrient compositions may exhibit substantially different thermal responses, particularly in terms of texture development. Third, the geometry of the printed food plays a critical role in radiative and conductive heat transfer during cooking. Designs with thinner cross-sectional areas or varying infill densities may respond differently under equivalent thermal conditions. Last, this study did not include sensory or consumer testing. Since consumer acceptance of novel food technologies—such as laser cooking—is pivotal for broader adoption, future work must incorporate organoleptic evaluation.

Consumer preferences for food mouthfeel can be very subjective (Jeltema et al., 2016). Laser-based texturization techniques would therefore benefit from integration with sensory panels to optimize cooking parameters according to user-centric preferences. The ability to customize food texture may enhance palatability and increase consumer willingness to consume novel or reformulated foods as a result (Kamei et al., 2024). Tailored texture control could have wide-reaching implications: improving the mouthfeel of softer foods to address sensory or functional deficits, enabling greater culinary creativity through spatially localized texture variation, and offering an alternative to bulk thermal processing methods that may reduce nutrient degradation.

Lasers are already recognized as a viable thermal processing method for achieving targeted texture, non-enzymatic browning (Blutinger et al., 2019a; Chen et al., 2019), and internal temperature control (Blutinger et al., 2021); but the nutritional implications of laser cooked foods remain largely unexplored. Understanding nutrient retention in lased foods is a critical next step—not only for informing consumer trust and regulatory guidance, but also for optimizing food quality and shelf-life. Future investigations could explore how ingredient composition (e.g., fat content, water activity, particle size) influences laser absorption and resultant texture; develop physics-based models to simulate the structural changes induced by laser exposure; and implement closed-loop systems using thermal imaging to dynamically adjust laser parameters and deliver user-defined texture profiles in real time.

4. Conclusions

Developing an appetizing and visually engaging 3D-printed meal is a multidimensional challenge, requiring the careful integration of all five senses into a single food item. While visual appeal may entice consumers, it is the flavor and texture that leave a lasting impression. These sensory elements must therefore be meticulously tailored to individual preferences to maximize satisfaction.

In this study, we have demonstrated the texturization capabilities of laser cooking technology and compared it to oven baking as a thermal processing method. Although textural development varied across strain regions, we successfully showcased the selective cooking potential of laser processing by employing different wavelengths of light and exposure levels. This research establishes a benchmark for future studies on selective cooking and food texturization, where further investigation is required.

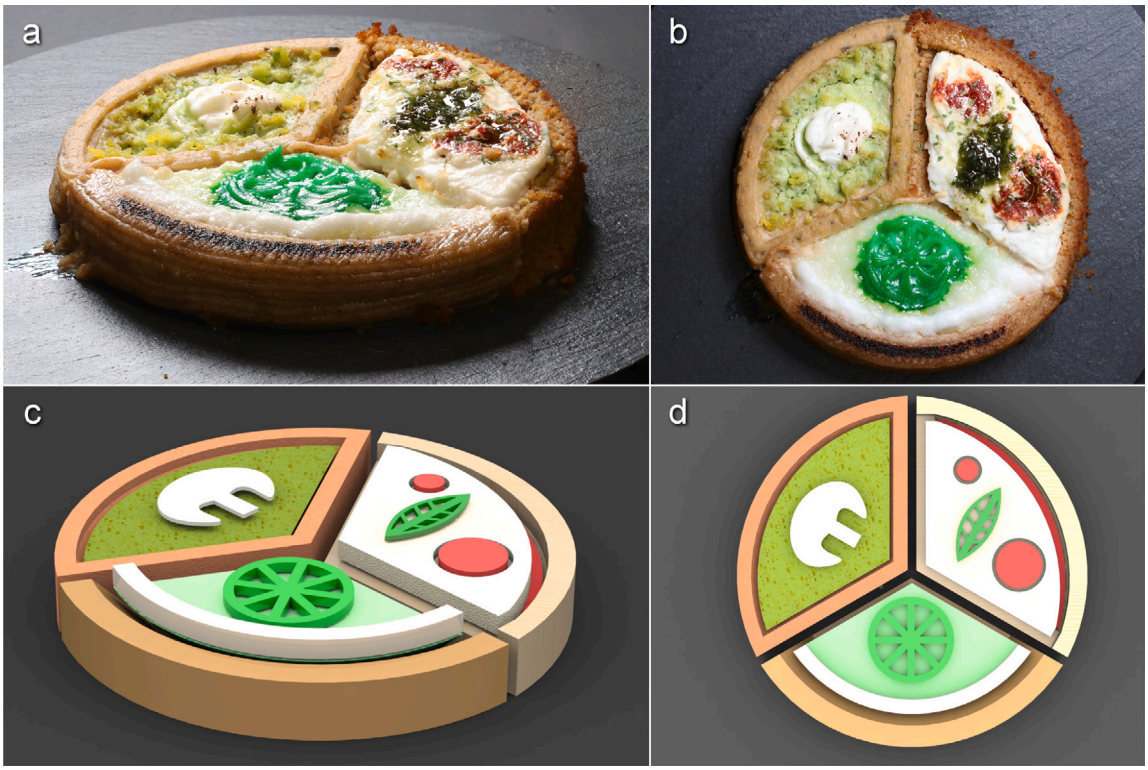

Fig. 5. A 3D-printed 14-ingredient 3-course meal. **a**, **b** Isometric view and top view of the final printed meal, respectively. **c**, **d** Isometric and top view of the computer-generated digital rendering, respectively.

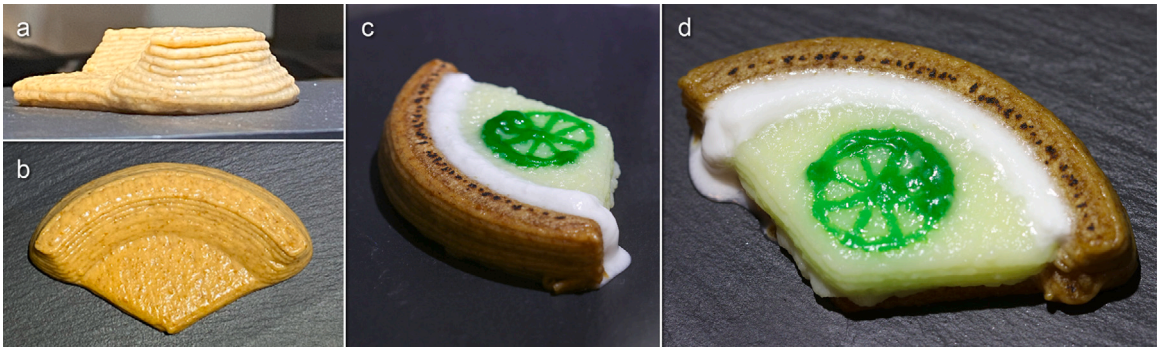

Fig. 6. Effects of laser cooking on the geometry of graham cracker crust. **a**, **b** Side and top view of raw 3D-printed graham cracker paste, respectively. **c**, **d** Side and top view of 3D-printed key lime with *in situ* laser cooking via blue laser for the graham cracker layers, respectively.

Notably, laser cooking offers a unique advantage in fortifying 3D-printed food structures during cooking, helping to preserve the integrity of the intended digital twin. Combining laser cooking with a bulk heating source, such as convection or conduction, may yield a more versatile cooking process, enabling customizable Maillard browning and precise textural expression. This hybrid approach holds promise for advancing the design and culinary potential of 3D-printed foods.

CRediT authorship contribution statement

Jonathan David Blutinger: Writing – review & editing, Writing – original draft, Validation, Supervision, Software, Project administration, Methodology, Investigation, Formal analysis, Data curation, Conceptualization. **Evan Lloyd Omo:** Validation, Formal analysis, Data curation. **Pol Bernat:** Validation, Formal analysis, Data curation. **Hod Lipson:** Writing – review & editing, Supervision, Project administration, Conceptualization.

Declaration of Generative AI and AI-assisted technologies in the writing process

During the preparation of this work the authors used ChatGPT in order to edit grammar and assist with data processing. After using this tool/service, the authors reviewed and edited the content as needed and take full responsibility for the content of the publication.

Declaration of competing interest

The authors declare the following financial interests/personal relationships which may be considered as potential competing interests: Jonathan Blutinger and Hod Lipson have patent issued to Columbia University in the City of New York. If there are other authors, they declare that they have no known competing financial interests or personal relationships that could have appeared to influence the work reported in this paper.

Acknowledgments

J.B. and H.L. were supported in part by the US National Science Foundation (NSF) AI Institute for Dynamic Systems (dynamicsai.org), grant 2112085, and by a grant from Redefine Meat Ltd. J.B. was also supported in part by the Oak Ridge Institute for Science and Education (ORISE).

Appendix A. Supplementary data

Supplementary material related to this article can be found online at https://doi.org/10.1016/j.jfoodeng.2025.112798.

Data availability

Data will be made available on request.

References

Ahrné, L., Andersson, C.-G., Floberg, P., Rosén, J., Lingnert, H., 2007. Effect of crust temperature and water content on acrylamide formation during baking of white bread: Steam and falling temperature baking. LWT-Food Sci. Technol. 40 (10), 1708–1715.

Almeida, E.L., Chang, Y.K., 2013. Structural changes in the dough during the pre-baking and re-baking of french bread made with whole wheat flour. Food Bioprocess Technol. 6, 2808–2819.

Home | BeeHex Automation, 2025. URL https://www.beehex.com/.

Blutinger, J.D., Cooper, C.C., Karthik, S., Tsai, A., Samarelli, N., Storvick, E., Seymour, G., Liu, E., Meijers, Y., Lipson, H., 2023. The future of software-controlled cooking. Npj Sci. Food 7 (1), 6.

Blutinger, J., Lipson, H., Meijers, Y., 2024. Method and systems for laser-based cooking. US Patent 11, 882, 859.

Blutinger, J.D., Meijers, Y., Chen, P.Y., Zheng, C., Grinspun, E., Lipson, H., 2018. Characterization of dough baked via blue laser. J. Food Eng. 232, 56–64.

Blutinger, J.D., Meijers, Y., Chen, P.Y., Zheng, C., Grinspun, E., Lipson, H., 2019a. Characterization of CO2 laser browning of dough. Innov. Food Sci. Emerg. Technol. 52, 145–157.

Blutinger, J.D., Meijers, Y., Lipson, H., 2019b. Selective laser broiling of atlantic salmon. Food Res. Int. 120, 196–208.

Blutinger, J.D., Tsai, A., Storvick, E., Seymour, G., Liu, E., Samarelli, N., Karthik, S., Meijers, Y., Lipson, H., 2021. Precision cooking for printed foods via multiwavelength lasers. Npj Sci. Food 5 (1), 24.

Chen, P.Y., Blutinger, J.D., Meijers, Y., Zheng, C., Grinspun, E., Lipson, H., 2019. Visual modeling of laser-induced dough browning. J. Food Eng. 243, 9–21.

Cheng, Y., Fu, Y., Ma, L., Yap, P.L., Losic, D., Wang, H., Zhang, Y., 2022. Rheology of edible food inks from 2D/3D/4D printing, and its role in future 5D/6D printing. Food Hydrocolloids 132, 107855.

Cheng, Y., Liang, K., Chen, Y., Gao, W., Kang, X., Li, T., Cui, B., 2023. Effect of molecular structure changes during starch gelatinization on its rheological and 3D printing properties. Food Hydrocolloids 137, 108364.

Christensen, C., 1984. Food texture perception. In: Advances in Food Research. Vol. 29, Elsevier, pp. 159–199.

Datta, A., Rakesh, V., 2013. Principles of microwave combination heating. Compr. Rev. Food Sci. Food Saf. 12 (1), 24–39.

De Grood, J.P.W., De Grood, P.J., 2013. Method and device for dispensing a liquid. US Patent 8, 556, 392.

Derossi, A., Caporizzi, R., Paolillo, M., Severini, C., 2021. Programmable texture properties of cereal-based snack mediated by 3D printing technology. J. Food Eng. 289, 110160.

Choc Edge - Creating Your Chocolate in Style, 2021. URL http://chocedge.com/.

Egbert-Jan, S., Vd Linden, D., Bommel, K.V., 2015. 3D food printing: The barilla collaboration. URL https://ec.europa.eu/jrc/sites/jrcsh/files/20150225-presentation-jan-sol.pdf.

Faridi, H., Faubion, J.M., 2012. Dough Rheology and Baked Product Texture. Springer Science & Business Media.

Home - Revo Foods, 2023. URL https://revo-foods.com/.

Fukuchi, K., Jo, K., Tomiyama, A., Takao, S., 2012. Laser cooking: a novel culinary technique for dry heating using a laser cutter and vision technology. In: Proceedings of the ACM Multimedia 2012 Workshop on Multimedia for Cooking and Eating Activities. pp. 55–58.

Gray, N., 2010. Looking to the future: Creating novel foods using 3D printing. Food Navig..

Hertafeld, E., Zhang, C., Jin, Z., Jakub, A., Russell, K., Lakehal, Y., Andreyeva, K., Bangalore, S.N., Mezquita, J., Blutinger, J., et al., 2019. Multi-material three-dimensional food printing with simultaneous infrared cooking. 3D Print. Addit. Manuf. 6 (1), 13–19.

Huang, M.-s., Zhang, M., Bhandari, B., 2019. Assessing the 3D printing precision and texture properties of brown rice induced by infill levels and printing variables. Food Bioprocess Technol. 12, 1185–1196.

Jaworska, D., Hoffmann, M., 2008. Relative importance of texture properties in the sensory quality and acceptance of commercial crispy products. J. Sci. Food Agric. 88 (10), 1804–1812.

Jeltema, M., Beckley, J., Vahalik, J., 2016. Food texture assessment and preference based on mouth behavior. Food Qual. Pref. 52, 160–171.

Kamei, M., Nishibe, M., Araki, R., Kohyama, K., Kusakabe, Y., 2024. Effect of texture preference on food texture perception: Exploring the role of matching food texture and preference. Appetite 192, 107078.

Liu, Z., Zhang, M., Bhandari, B., Wang, Y., 2017. 3D printing: Printing precision and application in food sector. Trends Food Sci. Technol. 69, 83–94.

Maldonado-Rosas, R., Tejada-Ortigoza, V., Cuan-Urquizo, E., Mendoza-Cachú, D., Morales-de La Pena, M., Alvarado-Orozco, J.M., Campanella, O.H., 2022. Evaluation of rheology and printability of 3D printing nutritious food with complex formulations. Addit. Manuf. 58, 103030.

Redefine Meat - New Meat, No Compromise, 2025. URL https://www.redefinemeat.com/.

Mondal, A., Datta, A., 2008. Bread baking–A review. J. Food Eng. 86 (4), 465–474.

Nashat, S., Abdullah, M., 2016. Quality evaluation of bakery products. In: Computer Vision Technology for Food Quality Evaluation. Elsevier, pp. 525–589.

Noort, M., Van Bommel, K., Renzetti, S., 2017. 3D-printed cereal foods. Cereal Foods World 62 (6), 272–277.

Pellegrino, R., Luckett, C.R., 2020. Aversive textures and their role in food rejection. J. Texture Stud. 51 (5), 733–741.

Periard, D., Schaal, N., Schaal, M., Malone, E., Lipson, H., 2007. Printing food. In: 2007 International Solid Freeform Fabrication Symposium.

Dream Pops | Plant-Based Desserts Coated in Chocolate!, 2022. URL https://dreampops.com/.

Cocoa Press 3D chocolate printer, 2025. URL https://cocoapress.com/.

Renzetti, S., Jurgens, A., 2016. Rheological and thermal behavior of food matrices during processing and storage: Relevance for textural and nutritional quality of food. Curr. Opin. Food Sci. 9, 117–125.

Scanlon, M., Zghal, M., 2001. Bread properties and crumb structure. Food Res. Int. 34 (10), 841–864.

Spence, C., Motoki, K., Petit, O., 2022. Factors influencing the visual deliciousness/eye-appeal of food. Food Qual. Pref. 102, 104672.

Stokes, J.R., Boehm, M.W., Baier, S.K., 2013. Oral processing, texture and mouthfeel: From rheology to tribology and beyond. Curr. Opin. Colloid Interface Sci. 18 (4), 349–359.

Suzuki, S., Cross, L., O'Doherty, J.P., 2017. Elucidating the underlying components of food valuation in the human orbitofrontal cortex. Nature Neurosci. 20 (12), 1780–1786.

Tang, D.W., Fellows, L.K., Dagher, A., 2014. Behavioral and neural valuation of foods is driven by implicit knowledge of caloric content. Psychol. Sci. 25 (12), 2168–2176.

Nourished US | Personalized 3D Printed Vitamins, 2025. URL https://us.getnourished.com/?gclsrc=aw.ds&&tw_source=google&tw_adid=666109092717&tw_campaign=20381027939&gad=1&gclid=Cj0KCQjwpc-oBhCGARIsAH6ote9JbuN-zErnbTgNJf_s9s3A4iVi8wAhGvXZeCK4PV2pm1OiSVOHG0gaAkIJEALw_wcB.

Wilkinson, C., Dijksterhuis, G., Minekus, M., 2000. From food structure to texture. Trends Food Sci. Technol. 11 (12), 442–450.

Willcocks, N.A., Shastry, A., Collins, T.M., Camporini, A.V., Suttle, J.M., 2011. High resolution ink-jet printing on edibles and products made. US Patent 7, 884, 953.

Zhang, B., Nasereddin, J., McDonagh, T., von Zeppelin, D., Gleadall, A., Alqahtani, F., Bibb, R., Belton, P., Qi, S., 2021. Effects of porosity on drug release kinetics of swellable and erodible porous pharmaceutical solid dosage forms fabricated by hot melt droplet deposition 3D printing. Int. J. Pharm. 604, 120626.

Zhang, L., Noort, M., van Bommel, K., 2022. Towards the creation of personalized bakery products using 3D food printing. In: Advances in Food and Nutrition Research. Vol. 99, Elsevier, pp. 1–35.

Zhu, S., Stieger, M.A., van der Goot, A.J., Schutyser, M.A., 2019. Extrusion-based 3D printing of food pastes: Correlating rheological properties with printing behaviour. Innov. Food Sci. Emerg. Technol. 58, 102214.

Zoran, A., 2019. Cooking with computers: The vision of digital gastronomy [point of view]. Proc. IEEE 107 (8), 1467–1473.